FIELD OBSERVATIONS OF STEP DYNAMICS ON A MACROTIDAL GRAVEL BEACH

Daniel Buscombe[1], Martin J. Austin[2], Gerhard Masselink[3]

1. School of Geography, University of Plymouth, Drake Circus, Plymouth PL4 8AA. daniel.buscombe@plymouth.ac.uk
2. School of Earth, Ocean and Environmental Sciences, University of Plymouth, Drake Circus, Plymouth PL4 8AA. martin.austin@plymouth.ac.uk
3. School of Geography, University of Plymouth, Drake Circus, Plymouth PL4 8AA. gerd.masselink@plymouth.ac.uk

Abstract: A data set consisting of detailed measurements of the hydrodynamics, morphological and sedimentological change, and sediment transport, has been collected from the region of the beach step on a macrotidal gravel beach. The step is an accretionary feature which evolves with a different relaxation time to that of the berm. Initiation of the step requires relative tidal stationarity and is thought to be triggered by increasingly reflective conditions. Despite its location, the step has remarkably stable sedimentology, differentiated from the swash zone using sedimentary moments. Co-spectral analysis indicates that sediment transport in the region of the step is related to sub-incident wave frequencies. A reconstructed ensemble sediment transport event confirmed that sediment transport at the base of the step occurs as a negatively skewed wave, perhaps sensitive to wave groups. The transition matrix of the nearshore gravel bed motion data closely resembled that of a 'memoryless' queuing process.

INTRODUCTION

The step is a common feature on reflective coarse-grained sand and gravel beaches (Bauer and Allen, 1995). The presence of the step imposes a steep hydrodynamic gradient across the nearshore which controls wave breaking. In fact, the beach step has been considered analogous to a breakpoint bar common to sand beaches

(Buscombe and Masselink, 2006), which would imply it was a region of on/offshore sediment convergence. As well as controlling wave breaking, the importance of the step lies in the fact that it is a beach protective feature, providing a locally steepening the active beachface, thus maintaining reflectivity during storms (Hughes and Cowell, 1987). It is able to do this because it is remarkably responsive to the semi-diurnal tidal cycle (Strahler, 1966; Miller and Ziegler, 1958), even on macrotidal beaches. The lack of previous studies into beach step dynamics belittles its importance, and belies the fact that it is an interesting case study for coarse-grain beach morpho-sedimentary-dynamics. We sought to redress this fact by carrying out a series of detailed field experiments, taking a holistic approach to the step with context to its evolving hinterland, and measuring hydrodynamic forcing, morphological and sedimentological change, and sediment transport.

FIELD EXPERIMENT AND METHODS

A field experiment was carried out on 27th September 2005 at Slapton, a 4 km-long macrotidal gravel barrier beach in Devon, UK. According to the Jennings and Shulmeister (2002) classification scheme, Slapton is a 'pure' gravel beach morphotype. During the measurement period the intertidal gradient was tan β=0.23 (Fig. 1), with a median sediment size of ~6mm. For a more detailed description of the field site refer to Austin and Masselink (2006a). The aim was to collect high-resolution concurrent and co-located morphological, sedimentological and hydrodynamic data from the step region as it evolved over a 6 hour period around high tide (+/- 3 hrs). The experiment was one of a three similar experiments within a wider morpho-sedimentary monitoring campaign of Slapton, 16-30th September 2005 on a spring-spring tidal cycle. The 27th September data set was the most comprehensive, and coincided with a period of major berm building just after neap tide (Fig. 1). Until this time the beach had been morphologically relatively inactive (Fig. 1). This is the first time measurements of each hydro-, morpho-, and morpho-sedimentary-dynamics have been made in the field across the step on a gravel beach.

Two instrument rigs were deployed aligned cross-shore. The first maintained a pressure transducer (PT) and a bi-directional electromagnetic current meter (ECM) measuring water depth and cross-shore and alongshore velocity respectively, logging at 16Hz 3cm above the bed around mid-step position. The second was located at the base of the step and measured velocity at 0.1, 0.25 and 0.4 m above the bed with a vertical array of Acoustic Döppler Velocimeters (ADVs), logging at 32Hz, and an ECM logging at 16Hz. An underwater colour digital video camera was also located here to observe the bed, logging at 25Hz. Swash excursion was measured using an electrical resistance wire maintained at 2cm above the bed, logging at 16Hz. Morphological measurements were made every 5 minutes across the foreshore and nearshore beyond the base of the step using Sallenger and Richmond's (1984) rapid profile technique. In addition, manual sediment samples taken at regular 5 minute intervals on the foreshore, to be dried and sieved at 1/4Φ. An additional video camera recorded the entire experiment from an oblique position just beyond the berm crest.

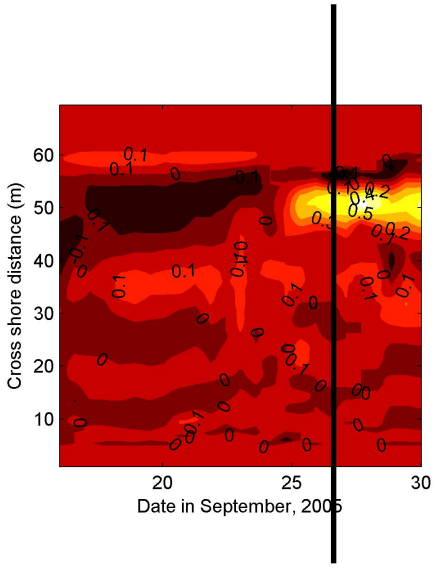

Fig (1) The antecedent morphological conditions prior to the experiment on the 27th (solid line) showing profile change (cm) relative to initial.

The size of gravel clasts and nature of gravel sediment transport precludes the use of optical and acoustic backscatter sensors to quantify sediment flux in the nearshore, which occurs almost exclusively as bedload and sheetflow. Instead, the underwater video was used as a measurement tool to quantify the magnitude of sediment transport (e.g. Williams, 1990; Stive et al. 2005). The video was decompiled into individual frames, converted to greyscale, and filtered for various sources to noise using powerful relaxed median (e.g. Hamza et al., 1999) and complex-valued log Gabor wavelet (Kovesi, 1999) filters. A two-dimensional correlation was applied between each consecutive frame, the reciprocal of which proved useful as a dimensionless 'bed motion coefficient', Ω sensitive to changes in bed 'texture' or gross (non-directional) bed mobility.

$$1/\Omega = \frac{\sum_m \sum_n \alpha\beta}{\sqrt{\sum_m \sum_n (\alpha)^2 \; - \; \sum_m \sum_n (\beta)^2}} \quad (1)$$

where m and n denote dimensions of image ι, $\alpha = {}_{mn}(t) - \acute{\iota}_{mn}(t)$ and $\beta = {}_{mn}(t+1) - \acute{\iota}_{mn}(t+1)$ where the over-dash denotes mean and t denotes time. High values of Ω indicate poorer correlation, therefore most change, and most sediment transport.

RESULTS

Hydrodynamics

Figure 2 summarises the hydrodynamic forcing derived from the pressure record. Water depth varied by c. 0.75m on a slightly asymmetrical neap tide, wave height was maintained between 0.5 and 0.6m, and spectral wave period increased from c. 5 to 10s. The trend in wave skewness (Elgar and Guza, 1985) was one of increasingly negative skew, and the spectral wave field displayed two prominent peaks at 5 and 12 seconds, the relative prominence of the latter increasing with time. Directional deviations away from shore-normal were uncommon and unsustained.

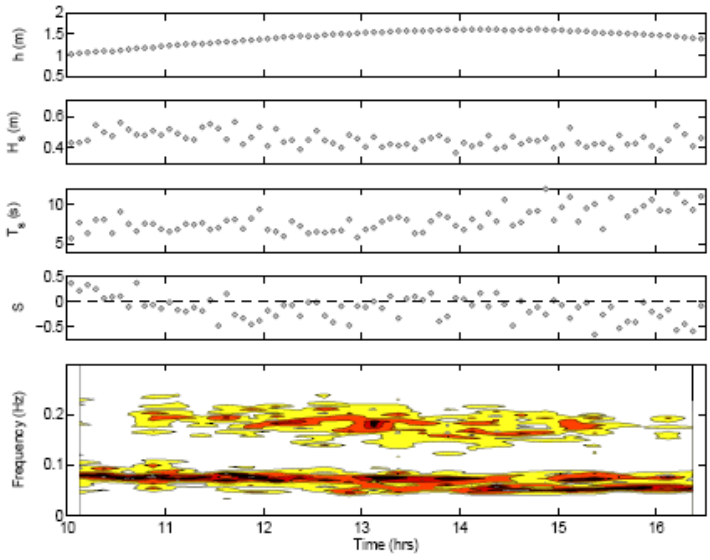

Fig (2). Hydrodynamic summary. Left panel (from top to bottom): water depth (m), significant wave height (m), significant wave period (s), wave skewness, and normalised spectral density (Hz m^2).

Morphodynamics

The pressure record was used to derived the surf scaling ε (Guza and Inman, 1975) and surf similarity ξ (Battjes, 1974) morphodynamic parameters for each 5 minute interval, using the 'active' intertidal slope, defined as the region of beachface between the 2% and 80% runup exceedance limits, measured with the resistance wire. The tidal translation rate (TTR) was calculated as the change in the 2% runup exceedance over consecutive 5 minute periods. The variation in these measures over the survey period may be seen in Fig. 3, where the period 10.45 – 11.30 has been highlighted since it was at this time that wave breaking regime moved from one of plunging/surging to fully surging. In the absence of significant change in wave steepness at this time, this change would have come about because the rising tide was advecting up an increasingly steep concave beach profile, making conditions more reflective. The surf scaling and similarity parameters
are generally agreed to be taxonomic for sand beach morphodynamic state, but in the relative scarcity of a gravel beach studies it was thought prudent to substantiate and validate the use surf similarity parameter to predict wave breaking on gravel beaches through independent means. Breakers were thus classified 'wave-by-wave' visually using the subaerial video record, and it was found that the agreement between visual observations and ξ was excellent. The wave breaker regime derived using visual observations from the video record is shown in the right panel of Fig. 3 (left), which shows the change in wave breaker type over the period 10.10 – 11.40, showing a marked transition between plunging and surging breaker types just before 11.00.

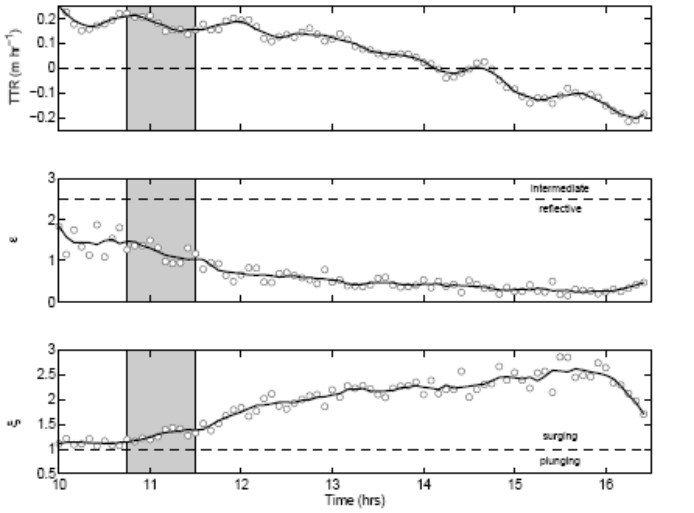

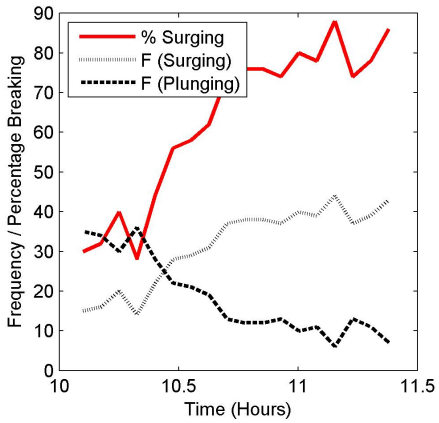

Fig (3). Left, from top to bottom: tidal translation rate (m hr^{-1}), surf scaling, and surf similarity. Grey patches on the right panels indicate the period 10.45 - 11.30 a.m. The solid black lines are a 5 point (25 minute) moving average. Right: changing wave breaker conditions based on video observations when step-berm morphologies begin to take hold.

A morphodynamic 'trigger' mechanism seems to control step initiation. Here, any causative relationships dictate that timing is crucial, i.e. whether the step begins to build before or after the change in wave breaking. If the step forms before the change in breaker type from plunging to surging, then that would be the necessary increase in slope to affect ξ, yet if the wave breaker transition precedes step formation then it is more likely that tidal excursion over a concave slope is key. The development of the step does not begin until after 11 a.m, by which time the change in hydrodynamic forcing has occurred.

Morphological change relative to initial was computed for every 5 minute survey of the beachface and nearshore, and the results are shown in the left panel of Fig. 4 (figures are in centimetres, therefore lighter shading represents relative accretion). The berm (at c. 53-50m) and step (at c. 58-56m) are clearly accretionary features, distinct from 'erosive' regions in the mid-swash (c. 56-53m) and nearshore (> 58m). Over the measurement period there is a net increase of 1.4 m^2 over each unit metre of beachface (contributed to predominantly by the berm). Incidentally, berm formation coincides almost exactly with the changing breaker regime, and we have no reason to suppose that berm formation did not occur according to onshore swash asymmetry overtopping mechanisms of Hine (1979); Austin and Masselink (2006); and Weir et al. (2006), since gross morphological change is consistent with these earlier findings. The step and berm are effectively independent features forced by discordant timescales: the relaxation time of the berm is linked with spring-neap tidal cycle (Fig 1), whereas the relaxation time of step is linked with semi-diurnal tidal cycle, and relative tidal stationarity (Fig. 4), and with the mid-foreshore remaining a morphological 'pivot point'. With this latter point in mind, there is little evidence to support the notion that the step forms due to an onshore/offshore convergence of sedimentation (e.g. Miller and Ziegler, 1958).

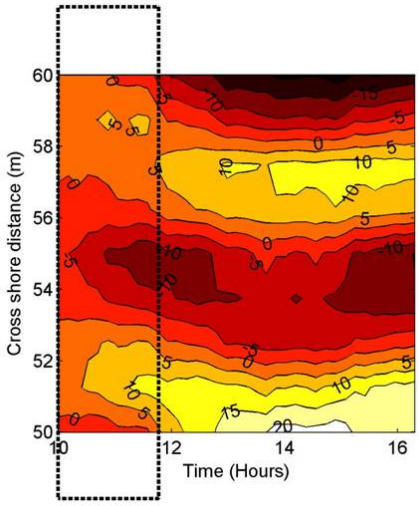

Fig (4) Morphological change, in cm, relative to initial (left panel) across the nearshore (seawards up the page) – light areas indicate accretion, dark depletion

Sediment Dynamics

The reported persistence of predominantly coarse sediments at the beach step (Miller and Ziegler, 1958; Bauer and Allen, 1995) dictates that the spatial and temporal characteristics of sediment size may have an important morphodynamic role, especially on gravel beaches (Sherman et al., 1993; Buscombe and Masselink, 2006) where the range of sediment size is so large. Spatial patterns of morpho-sedimentary variation are mixed over the entire foreshore (Fig. 5, both panels). Coarsening is associated with the development of step and berm features, but also with the depletion of material in the nearshore. Fining is associated with the upper

foreshore, co-incident with removal of material, and step crest which is coincident with the deposition of material (Fig. 5, both panels). In a gross sense, each hydro-kinematic region thus has a distinct 'morpho-sedimentary domain', so it is possible to trace the gross trend of berm and step building-coarsening through time, and it may be seen that the mid-foreshore is a sedimentological as well as morphological pivot point. By contrast, the time-averaged grain size distribution remains relatively unchanged (i.e. no temporal trend).

Figure 6 reveals that step sediments are characteristically coarser skewed, more poorly sorted, and more platykurtic, than the sediments of the foreshore and berm. Despite the location of the step, it has remarkably stable sedimentology, and it is thus possible to distinguish the step from the foreshore using sedimentary moments.

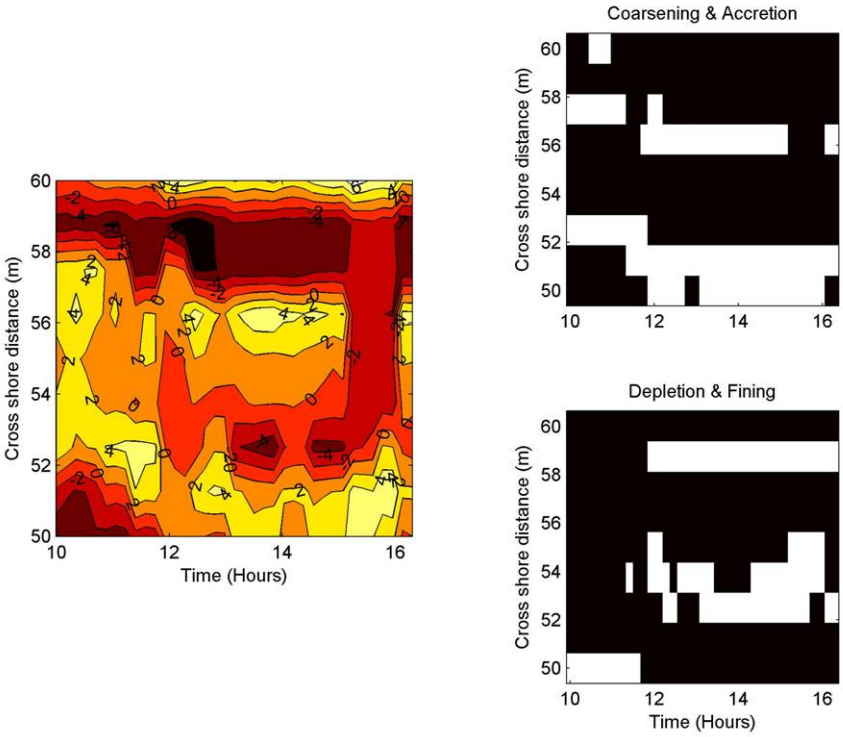

Fig (5) Sedimentological change (left panel), in mm, relative to mean size profile (lighter shading indicates coarsening); regions of morpho-sedimentary co-variation (right panels) – coexistence of relative sediment accretion and coarsening (top), and relative sediment depletion and fining (bottom).

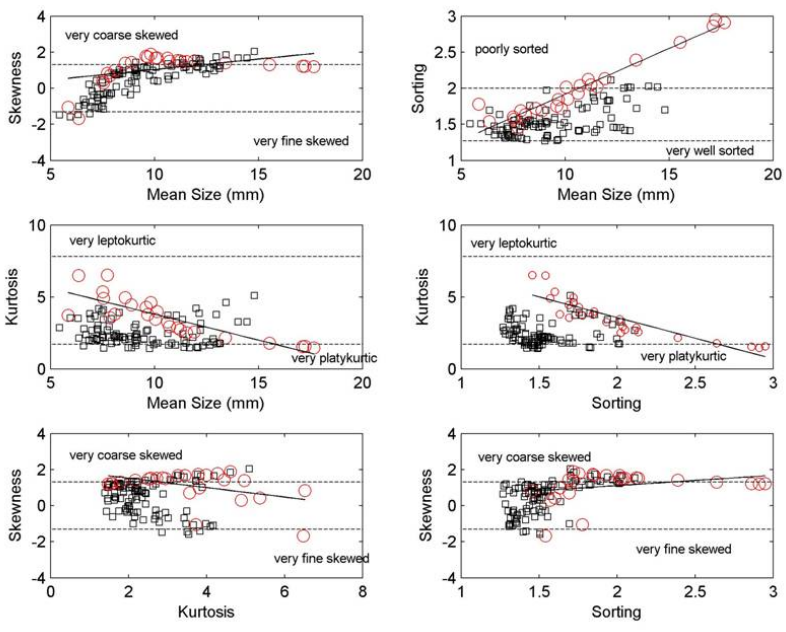

Fig (6) Bivariate scatterplots of geometric moments for swash/berm (black squares) and step (red circles) sediments. Solid lines show linear least squares fits through the step data; dashed lines show dependent variable classification boundaries (Folk and Ward, 1957).

Sediment Transport

The limited amount of work which has quantified transport of gravel-sized sediment in coastal environments has been shown transport to be a highly irregular function of instantaneous fluid forcing and mechanistic properties of the bed. Heathershaw and Thorne (1985) demonstrated that the majority of gravel sediment transport under tidal currents occurs as short duration, turbulent and particular events, un-related to time-averaged flow parameters. Further work by Thorne (1986b), Williams (1990), Hardisty (1991) and others (generally in deeper water) demonstrated the role particle inertia and the various mechanical properties of the bed may have to play on the (therefore highly nonlinear) response of natural gravel sediments to nearshore flow velocity. What is clear from this work is that gravel sediment transport is dependent on both deterministic (e.g. oscillatory and mean flow velocities), and probabilistic phenomena (e.g. bed configurations, sediment properties, turbulence), but little work has been carried out to quantify sediment transport in the nearshore because of the measurement difficulties associated with such work. Recent researchers have emphasised the role of fluid accelerations (and associated horizontal pressure gradients) on coarse particle transport (e.g., Drake and Calantoni, 2001; Hoefel and Elgar, 2003; Stive et al., 2005).

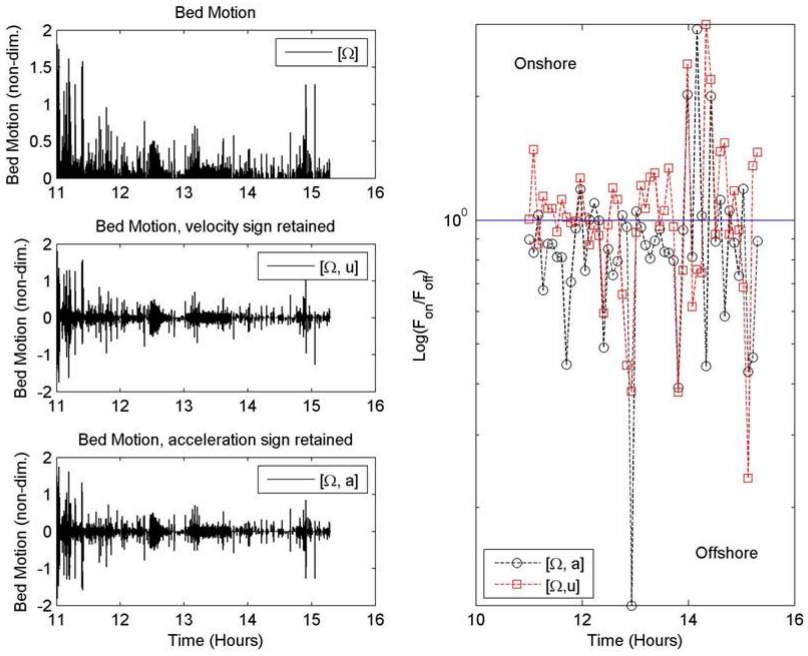

Fig (7). Magnitude-response diagram for Ω. The original time series of Ω is depicted in the upper left panel; the middle left panel shows Ω magnitude with the instantaneous directional component of velocity retained; and the lower left panel shows Ω magnitude with the instantaneous directional component of velocity acceleration retained. The right panel shows normalised bed motion magnitude (see text) for acceleration (black circles) and velocity (red squares).

The bed motion data was re-sampled to 4Hz to correspond with the velocity sample frequency. Upon visual inspection there was systematic bed motion response to neither velocity direction nor magnitude; acceleration direction nor magnitude. Indeed, bed motion induced by similar velocity or acceleration events was often very different in duration and magnitude. Assuming instantaneous sediment transport response to nearshore fluid motions, the sign of Ω was scaled according to the instantaneous directional component of velocity and acceleration (i.e. positive onshore, negative offshore), to yield $+/-\Omega_u$ and $+/-\Omega_a$ respectively, and the following calculations were performed for each 5 minute segment of data:

$$\delta_a = \log\left(\frac{\sum|\Omega_a|}{\sum|-\Omega_a|}\right); \quad \delta_u = \log\left(\frac{\sum|\Omega_u|}{\sum|-\Omega_u|}\right) \tag{2}$$

providing a ratio of time-averaged onshore:offshore dimensionless sediment flux, assuming instantaneous response to fluid forcing. Fig. 7 (right) shows these ratios over time, showing that in general values lie close to unity, however in general in can be seen that sediment flux which occurs when flows are accelerating offshore is greater than sediment flux which occurs when flows are accelerating onshore. Conversely, sediment flux is greater when velocity is directed onshore.

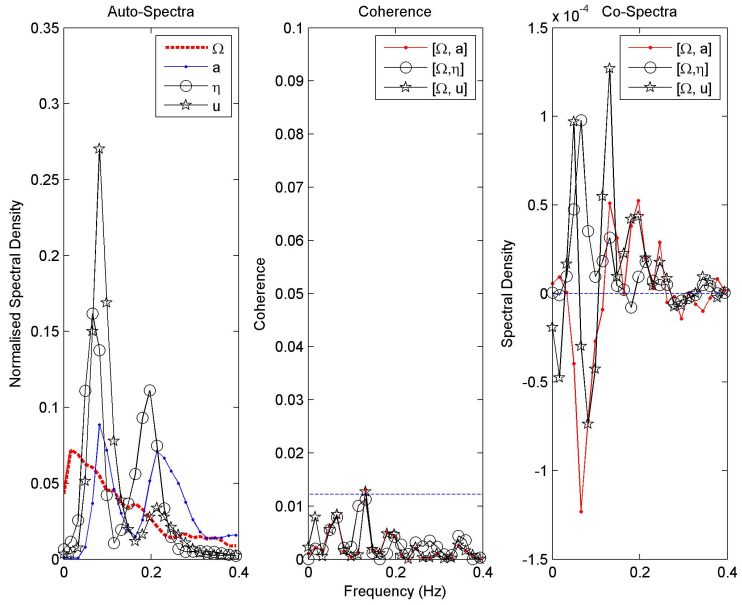

Fig (8) Spectral analysis of *u, a, η* and *Ω*. Left panel: autospectra of *Ω* (non-dim. Hz^{-1}) shown as red dashed line; *η* (m^2 Hz^{-1}) as open circles; *u* (ms^{-1} Hz^{-1}) as open stars; and *a* (ms^2 Hz^{-1}) as blue dots (note that the auto-spectra have been normalised by their total variance, e.g. m^2 $Hz^{-1}/\Sigma m^2$ Hz^{-1} for *η*). Middle panel: cross-spectral coherence (the dashed line is the 95% confidence interval) for [*Ω, a*], [*Ω,u*], and [*Ω, η*] denoted as red dots, open circles and stars respectively. Right panel: co-spectra for [*Ω, a*], [*Ω,u*], and [*Ω, η*] denoted as red dots, open circles and stars respectively

Figure 8 shows the spectral characteristics of the bed motion (Ω, Eq. 1) surface elevation (*η*), cross-shore current velocity (*u*) and cross-shore current acceleration (*a*). Auto-spectra for Ω showed peaks at low frequencies (0.03-0.05Hz), compared to the corresponding spectra of *u* and *a* which showed peaks at 0.08 and 0.2 Hz. These spectral peaks indicate a wave field composed of 12 and 5 second period waves, travelling in groups with a period of approximately 33 seconds. Cross correlation between the velocity envelope and a lowpass-filtered Ω (not shown – refer to Austin and Buscombe, *submitted*) shown a highly significant positive correlation at ~5 second lag. This could suggest that sediments respond strongest to sub-incident wave frequencies, which could mean that individual waves stir/destabilise sediments, and the largest wave(s) in a group carry out most of the transportation. Equally, it could indicate that the importance of the magnitude of the velocity event which transports most sediment is diminished, if the *sequence* of individual waves which are large enough to stir the bed is long enough. In which case, stress 'histories' are more important in the movement of clasts than instantaneous bed stresses (Paphitis and Collins, 2005).

Co-spectral analysis between *Ω* and *u* (e.g., Huntley and Hanes, 1987) showed very poor coherence and significance over the frequencies of interest (Fig. 8). Low coherence between velocity and transport suggests transport is highly intermittent,

highly variable at swell frequencies, and clearly a highly non-linear function of flow velocity.

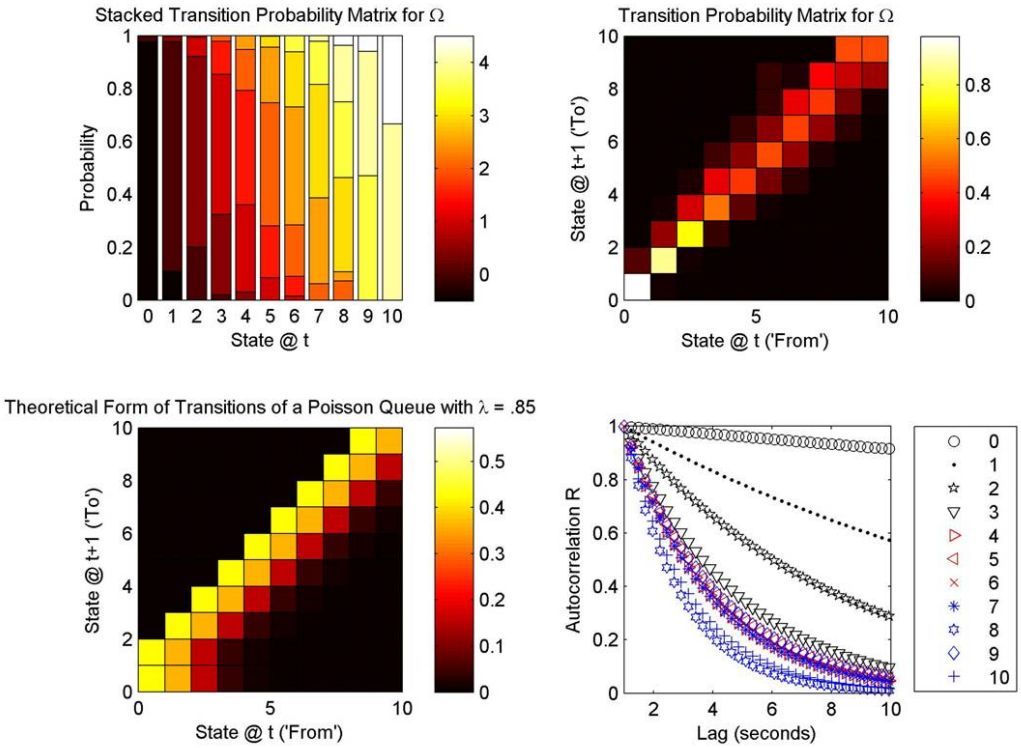

Fig (10) Sediment transport as a Markov chain: transition probability matrix for Ω_{rr} (top panels); autocorrelation functions, R, for Ω_{rr} states (bottom panels)

In order to glean further information about the nature of bed motion, the data was analysed further using a probabilistic model in order to reconstruct an ensemble or 'typical' transport event. Dimensionless raw Ω was linearly rescaled to span the interval 0-10, and rounded to the nearest integer in order to obtain a discrete record Ω_{rr} which maintained similar resolution. A transition probability matrix (TPM) of the Ω_{rr} data was constructed (Fig. 10), and using Markov Chain theory (e.g., Kemeny and Snell, 1976), analysed for its general distributional form and persistence characteristics.

With reference to the TPM for Ω in Fig. 10, the absence of transitional extremes validates the sample frequency at which the data was collected. The transition matrix shows that sediment transport 'events' are in general negatively skewed. For example, the transition probabilities are not symmetrical about the inertial left-right diagonal, and the probability for an event of *increased* magnitude to follow an event of *given* magnitude is larger than the vice-versa (i.e. incline tendencies). Specifically, values of average magnitude have a larger transitional spread; therefore the skew in the wave will not be drawn by the mode (event peak) or tails but by the falling limb. In order to reconstruct the ensemble event the remaining information required is the persistence characteristics of every magnitude. The rank autocorrelation function of a Markov chain is given by (Basawa, 1972):

$$R = \frac{\sum_{i,j} ij\Theta_{ij} - \left(\sum_{i,j} i\Theta_{ij}\right)^2}{\sum i^2\Theta_{ij} - \left(\sum_{i,j} i\Theta_{ij}\right)^2} \tag{3}$$

where $\Xi_{ij} = \pi^T P^T$ such that $\Sigma_{ij}\Xi_{ij} = 1$, and where *T*, *i*, *j*, *P*, and π denote matrix transpose, row, column, transition matrix, and steady state probability vector, respectively. The steady state vector is found by solving the set of equations:

$$\pi = P\pi \tag{4}$$

subject to $\Sigma\pi = 1$. The autocorrelation functions for each magnitude are shown in Figure 10 (bottom right panel), showing an almost linear decrease in persistence with increasing magnitude. What this means in a physical sense is that a typical sediment transport event resembles a negatively skewed wave which is composed of a series of steps of increasing shorter length. This general form complies with visual inspection of the data, and could be interpreted as the first waves in a group 'clearing' the bed of a certain proportion of movable grains, until a threshold is reached where the conditions have been primed for the greatest amount of transport, after which the bed is relatively immobile. This implies a great deal of initial resistance to movement imposed by the micro-mechanical configurations of the bed (temporal and spatial distributions of grain size, 'hiding' factors, relative flow protrusion, etc).

The transition matrix for Ω (Fig. 10) resembled the theoretical form of a 'memoryless' Poisson queuing process, given by;

$$P_n(t) = e^{-\lambda t}\frac{(\lambda t)^n}{n!} \tag{5}$$

which expresses the probability of an event n in time t given by average number of occurrences per unit time, λ such that there would be λt events on average in t, implying inter-arrival times are exponentially distributed by $e^{-\lambda t}$, and the average number of events is the same for each unit interval of t, which is the 'memoryless' property (e.g. Kleinrock, 1975). For example, the TPM associated with a Poisson queue controlled by arrival rate λ=0.85 is depicted in Fig. 10 (bottom left). This draws strong parallels with similar work carried out on gravel sediment transport in fluvial settings (e.g. Einstein, 1937; Hassan et al., 1991).

CONCLUSION

The gravel beach step is an accretionary feature strongly linked to tidal stage, evolving with a different relaxation time to that of the berm. Initiation of step morphology requires tidal stationarity and is perhaps triggered by a change wave breaker type from plunging to surging. The beachface at short timescales is effectively a closed sedimentary unit although the step and beachface may be differentiated using sedimentary moments. Different morphological features such as the step have typical spatial sedimentary responses. Nearshore sediment transport is related to sub-incident frequencies (wave groups) but is not a linear function of either velocity magnitude or direction. Therefore, a better description of sediment transport requires instantaneous sediment size information, which has to be remotely sensed. It is possible to reconstruct an ensemble sediment transport event using the transitional properties of the data The transition matrix for bed motion resembled the theoretical form of a 'memoryless' Poisson queuing process.

ACKNOWLEDGEMENTS

Thanks to field assistants Tamsin Watt, Ben Allured, Jon Tinker, and George Graham. This work was funded by a faculty scholarship awarded to DB, and a post-graduate research grant awarded to MJA by the British Geomorphological Research Group. Thanks to Jon Tinker for improving the efficiency of the Markov chain computations.

REFERENCES

Austin, M.J., and Masselink, G. (2006a). "Observations of morphological change and sediment transport on a steep gravel beach," *Marine Geology* 229, 59-77.

Austin, M.J., and Buscombe, D. (submitted). "Morphological change and sediment dynamics of the beach step on a macrotidal gravel beach," *Marine Geology.*

Bauer, B.O., and Allen, J. (1995). "Beach steps: an evolutionary perspective," *Marine Geology* 123, 143-166.

Battjes, J.A. (1974). "Surf similarity," *Proceedings 14th International Conference on Coastal Engineering* pp. 466-480, ASCE.

Buscombe, D., and Masselink, G. (2006). "Concepts in gravel beach dynamics," *Earth Science Reviews* 79, 33-52.

Drake, T.G., and Calantoni, J. (2001). "Discrete particle model for sheet flow

sediment transport in the nearshore," *Journal of Geophysical Research* 106, 19859-19868.

Einstein, H.A., (1937). "*Bedload transport as a probability problem*," PhD Dissertation, Eidenoess. tech. Hochsch., Zurich, Switz. (English translation by W.W. Sayre, in "*Sedimentation"*, edited by H.W. Shen, Appendix C, H.W. Shen, Fort Collins, Colo., 1972).

Elgar, S., and Guza, R.T. (1985). "Observations of bispectra of shoaling surface gravity waves," *Journal of Fluid Mechanics* 161, 425-448.

Folk, R.L., and Ward, W.C. (1957). "Brazos River bar (Texas): a study in the significance of grain size parameters," *Journal of Sedimentary Research* 27, 3-26.

Guza, R.T., and Inman, D.L. (1975). "Edge waves and beach cusps," *Journal of Geophysical Research-Oceans* 80, 2997-3012.

Hamza, A.B., Luque-Escamilla, P.L., Aroza, J.M., and Roldan, R.R. (1999). "Removing noise and preserving details with relaxed median filters," *Journal of Mathematical Imaging and Vision* 11, 161-177.

Hassan, M.A., Church, M., and Schick, A.P. (1991). "Distance of movement of coarse particles in gravel bed streams," *Water Resources Research* 27, 503-511.

Heathershaw, A.D., and Thorne, P.D. (1985). "Sea bed noises reveal role of turbulent bursting phenomena in sediment transport by tidal currents," *Nature* 31, 339-342.

Hine, A.C. (1979). "Mechanisms for berm development and resulting beach growth along a barrier spit complex," *Sedimentology* 26, 333-351.

Hoefel, F., and Elgar, S. (2003). "Wave-induced sediment transport and sand bar migration," *Science* 299, 1885-1887.

Hughes, M., and Cowell, P. (1987). "Adjustment of reflective beaches to waves," *Journal of Coastal Research* 3, 153-167.

Huntley, D.A., and Hanes, D.M. (1987). "Direct measurement of suspended sediment transport," *Coastal Sediments '87*, pp. 723-737, ASCE.

Jennings, R., and Shulmeister, J. (2002). "A field based classification scheme for gravel beaches," *Marine Geology* 186, 211-228.

Kemeny, J.G, and Snell, J.L. (1976). "*Finite Markov Chains*, *2nd edition.*" Springer-Verlag, New York.

Kleinrock, L. (1975). *"Queueing Systems Volume 1: Theory."* Wiley Interscience, New York.

Kovesi, P. (1999). "Phase preserving de-noising of images," *The Australian Pattern Recognition Society Conference, DICTA'99*, pp. 47-67.

Miller, R.L., and Ziegler, J.M. (1958). "A model relating dynamics and sediment pattern in equilibrium in the region of shoaling waves, breaker zone, and foreshore," *Journal of Geology* 66, 417-441.

Paphitis, D., and Collins, M.B. (2005). "Sand grain threshold, in relation to bed 'stress history': an experimental study," *Sedimentology* 52, 827-838.

Sallenger, A.H., and Richmond, B.M. (1984). "High frequency sediment level oscillations in the swash zone," *Marine Geology* 60, 155-164.

Sherman, D.J., Orford, J.D., and Carter, R.W.G. (1993). "Development of cusp-related, gravel size and shape facies at Malin Head, Ireland," *Sedimentology* 40,

1139-1152.
Stive, M.J.F., Reniers, A.J.H.M., Terrile, E., and Verhagen, H.J. (2005). "Coarse particles' threshold of motion under shoaling waves," *Coastal Dynamics '05*, ASCE.
Strahler, A.N. (1966). "Tidal cycle of changes in an equilibrium beach Sandy Hook, New Jersey," *Journal of Geology* 74, 247-267.
Thorne, P.D. (1986b). "An intercomparison between visual and acoustic detection of seabed gravel movement," *Marine Geology* 72, 11-31.
Weir, F., Hughes, M., and Baldock, T.E. (2006). "Beachface and berm morphodynamics fronting a coastal lagoon," *Geomorphology* 82, 331-346.
Williams, J.J. (1990). "Video observations of marine gravel transport," *Geo-Marine Letters* 10, 1432-1157.